Rare Metal Materials and Engineering
Volume 54, Issue 4, April 2025
Available online at www.rmme.ac.cn

Science Press

Cite this article as: Long Weimin. Design Guidelines for Composition of Brazing Filler Metals and Evolution Mechanisms of Typical Microstructures[J]. Rare Metal Materials and Engineering, 2025, 54(04): 837-853.
DOI: https://doi.org/10.12442/j.issn.1002-185X.20250097.

EDITORIAL

Design Guidelines for Composition of Brazing Filler Metals and Evolution Mechanisms of Typical Microstructures

Long Weimin

State Key Laboratory of High Performance & Advanced Welding Materials, China Academy of Machinery Zhengzhou Research Institute of Mechanical Engineering Co., Ltd, Zhengzhou 450052, China

Abstract: Brazing filler metals are widely applied, which serve as an industrial adhesive in the joining of dissimilar structures. With the continuous emergence of new structures and materials, the demand for novel brazing filler metals is ever-increasing. It is of great significance to investigate the optimized composition design methods and to establish systematic design guidelines for brazing filler metals. This study elucidated the fundamental rules for the composition design of brazing filler metals from a three-dimensional perspective encompassing the basic properties of applied brazing filler metals, formability and processability, and overall cost. The basic properties of brazing filler metals refer to their mechanical properties, physicochemical properties, electromagnetic properties, corrosion resistance, and the wettability and fluidity during brazing. The formability and processability of brazing filler metals include the processes of smelting and casting, extrusion, rolling, drawing and ring-making, as well as the processes of granulation, powder production, and the molding of amorphous and microcrystalline structures. The cost of brazing filler metals corresponds to the sum of materials value and manufacturing cost. Improving the comprehensive properties of brazing filler metals requires a comprehensive and systematic consideration of design indicators. Highlighting the unique characteristics of brazing filler metals should focus on relevant technical indicators. Binary or ternary eutectic structures can effectively enhance the flow spreading ability of brazing filler metals, and solid solution structures contribute to the formability. By employing the proposed design guidelines, typical Ag based, Cu based, Zn based brazing filler metals, and Sn based solders were designed and successfully applied in major scientific and engineering projects.

Key words: design of brazing filler metals; design guidelines for composition; Ag based brazing filler metals; eutectic structures evolution

1 Introduction

The variety of brazing filler metals, each with distinct properties, primarily stems from the demands of brazing engineering and cost control. Since brazing is employed to address engineering challenges that other joining technologies struggle to solve, brazing filler metals are confronted with the complex design challenges of “multiple-variety”, “multi-property”, and “multi-manufacturing processes”[1].

“Multiple-variety” refers to the extensive range of chemical composition in brazing filler metals, with varying elemental ratios, promoting the continuous emergence of multiple-series brazing filler metals[2]. “Multiple-property” denotes the diversity in mechanical, physicochemical, and electromagnetic properties of brazing filler metals resulting from changes in their chemical compositions[3]. “Multiple-manufacturing processes” describes the preparation procedures and technologies designed to produce brazing filler metals in various shapes by employing metal forming techniques such as casting, forging, extrusion, rolling, drawing, shearing, and coiling to meet the requirements of brazing operations[4].

The brazing filler metals can be classified into three categories based on the analysis of internationally disclosed composition, including high-temperature, medium-temperature, and low-temperature filler metals. Among them, high-temperature brazing filler metals mainly include Ni based[5],

Received date: February 28, 2025
Foundation item: National Natural Science Foundation of China (U22A20191)
Corresponding author: Long Weimin, Ph. D., Professor, State Key Laboratory of High Performance & Advanced Welding Materials, China Academy of Machinery Zhengzhou Research Institute of Mechanical Engineering Co., Ltd, Zhengzhou 450052, P. R. China, E-mail: longwm@zrime.com.cn

Mn based[6], and Ti based filler metals[7]; medium-temperature brazing filler metals primarily consist of Cu based[8], Ag based[9], and Al based filler metals[10]; while low-temperature brazing filler metals are mainly Sn based[11], Zn based[12], and Au based filler metals[13]. The State Key Laboratory of High-Performance & Advanced Welding Materials at Zhengzhou Research Institute of Mechanical Engineering Co., Ltd (China) has manufactured over 1200 types of brazing filler metals, tested more than 1500 types of brazing filler metals, and documented over 3000 types of brazing filler metals in the literature, approximately half of which are similar-composition brazing filler metals produced by different institutions. Among these brazing filler metals, high-temperature filler metals are primarily used to braze superalloys[14], Ti alloys[15], refractory metals[16], and ceramics[17]. Medium-temperature filler metals are mainly employed to braze steel and stainless steel[18], copper and its alloys[19], cast iron[20], cemented carbide[21], aluminum and its alloys[22], and carbon-based materials[23]. Low-temperature filler metals have the widest range of applications and can be used to braze almost all structural and functional materials, including but not limited to electronic components, sensors, and light industrial products[24]. Due to the continuous emergence of new materials, structures, and functionalities, the composition design methods and technical pathways of brazing filler metals deserve further research.

2 Design Guidelines for Composition of Brazing Filler Metals

The design of brazing filler metals must achieve three fundamental objectives: the basic properties of the material, its manufacturability and operational applicability, and cost (Fig. 1). The basic properties of brazing filler metals encompass the mechanical properties of both the brazing filler metals and brazed joints, physical and chemical properties, electromagnetic properties, as well as adaptability to optical and nuclear environments. Manufacturability and operational applicability include the processability of brazing filler metals for hot forming and cold working, the achievability of shape and size specifications, as well as the requirements for addition of brazing filler metals during brazing. The processability of brazing mainly refers to wettability, castability, and spreadability. Cost is largely tied to the compositional elements, and for extreme-sized brazing filler metals, it is essential to account for the costs of manufacturing process.

2.1 Selection rules of brazing alloy systems for wettability

The selection of brazing alloy systems should be based on the physical, chemical, and metallurgical properties of the base materials to be joined. The alloying elements, particularly the primary and secondary major elements, must exhibit metallurgical compatibility with the base material. Ideally, they form a solid solution with the highest solubility. Alternatively, they form an intermetallic compounds (IMCs) with adequate strength and toughness. For instance, Qin et al[25] fabricated CuZnNiMn brazing filler metals to effectively

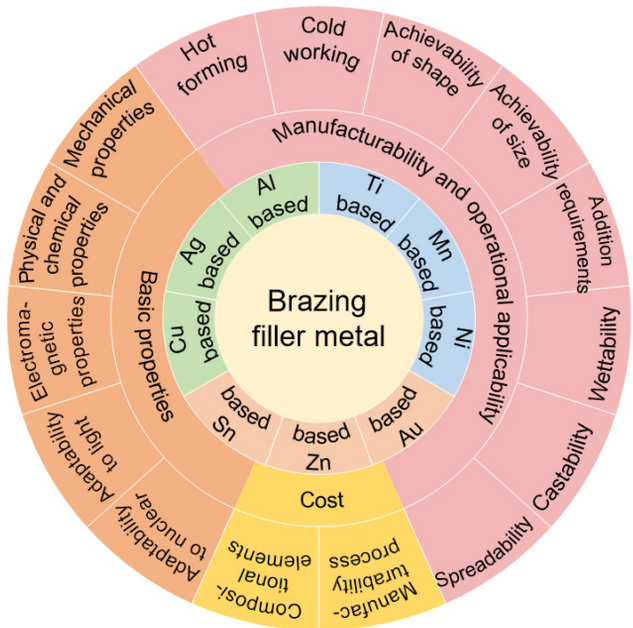

Fig.1 Design of composition of brazing filler metals

braze 42CrMo steel and YGB cemented carbide, and obtained brazed joints with shear strength exceeding 260 MPa and excellent gap filling capability. Based on the Cu-Fe and Fe-Zn binary phase diagrams (Fig. 2a – 2b). The Cu and Zn elements can both be solid-solved in the Fe matrix, and the Fe element can also be solid-solved in the Cu matrix. The microstructures in CuZnNiMn brazing filler metals mainly contained CuMn (α) and CuZn (β) solid solutions, as shown in Fig. 2c, and the Cu-Zn solid solution (β) was also formed between CuZnNiMn filler metals and 42CrMo steel, as shown in Fig. 2d. Therefore, the primary and secondary major elements had a good metallurgical compatibility with Fe matrix, conforming the selection rules of brazing alloys systems.

BAg30CuZnSn brazing filler metals, prepared by Shi et al[26], were utilized to successfully braze copper with excellent mechanical properties. The primary and secondary major elements in BAg30CuZnSn brazing filler metals were Ag and Cu, and the base material was copper. According to the Ag-Cu binary phase diagram (Fig.3a), Ag and Cu elements tended to form solid solutions, exhibiting good metallurgical compatibility. In our previous studies, the phases formed in BAg30CuZnSn brazing filler metals were determined to be Ag-rich, Cu-rich, and eutectic structures, as shown in Fig. 3b. The interfacial phase formed between brazing filler metals and base materials during brazing was Cu-rich solid solution containing Ag element, as shown in Fig.3c.

Long et al[27] designed an in-situ synthesized Al-Si-Cu brazing filler metal to braze 3A21 aluminum alloys, and obtained reliable brazed joints with high shear strength. For the Al-Si-Cu brazing filler metals, the Si element has a certain solubility in the Al matrix, based on the Al-Si binary phase diagram in Fig.4a. The microstructures mainly consisted of Al

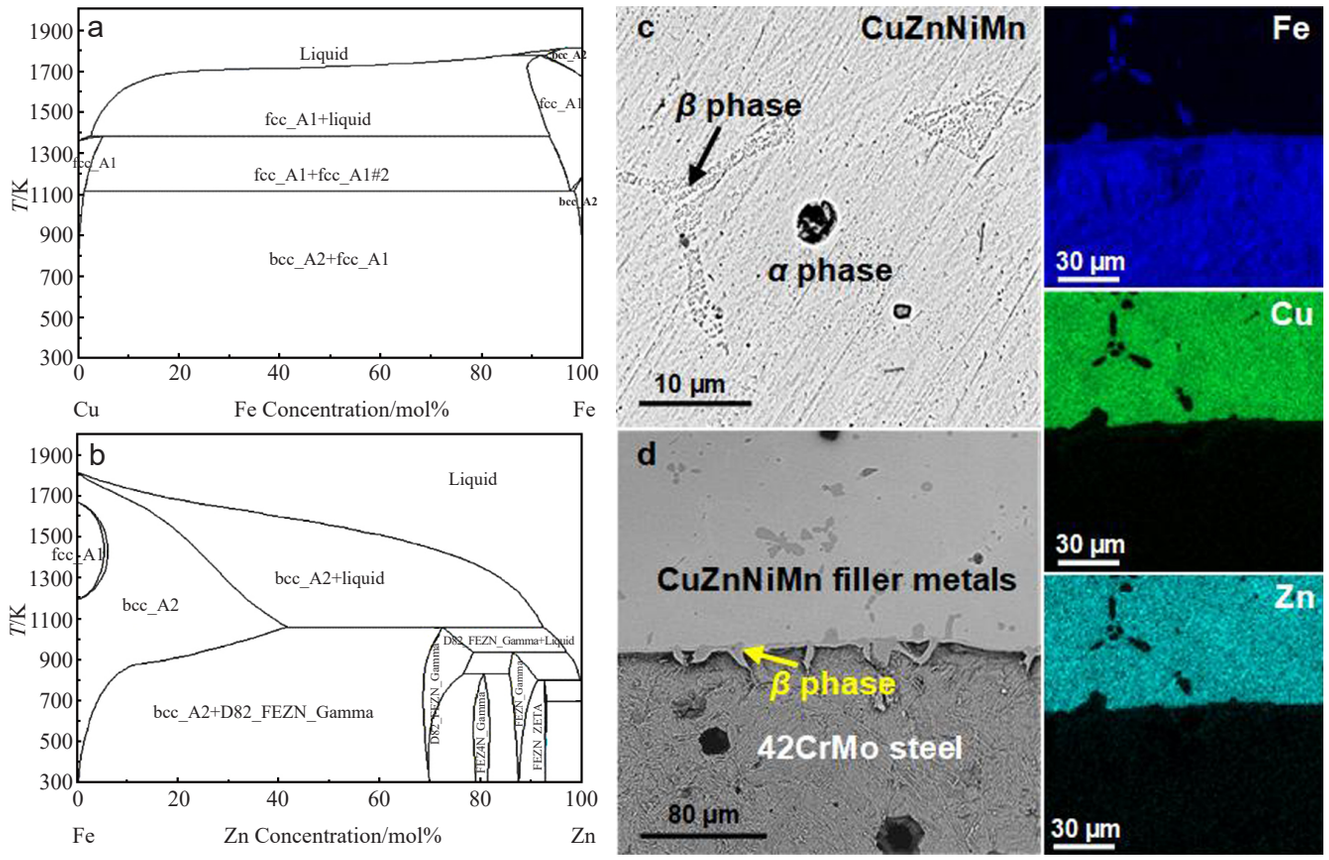

Fig.2 Cu-Fe (a) and Fe-Zn (b) binary phase diagrams; microstructure in the CuZnNiMn brazing filler metal (c); cross-sectional microstructure and elements distribution in the CuZnNiMn filler metal/42CrMo steel joint (d)[25]

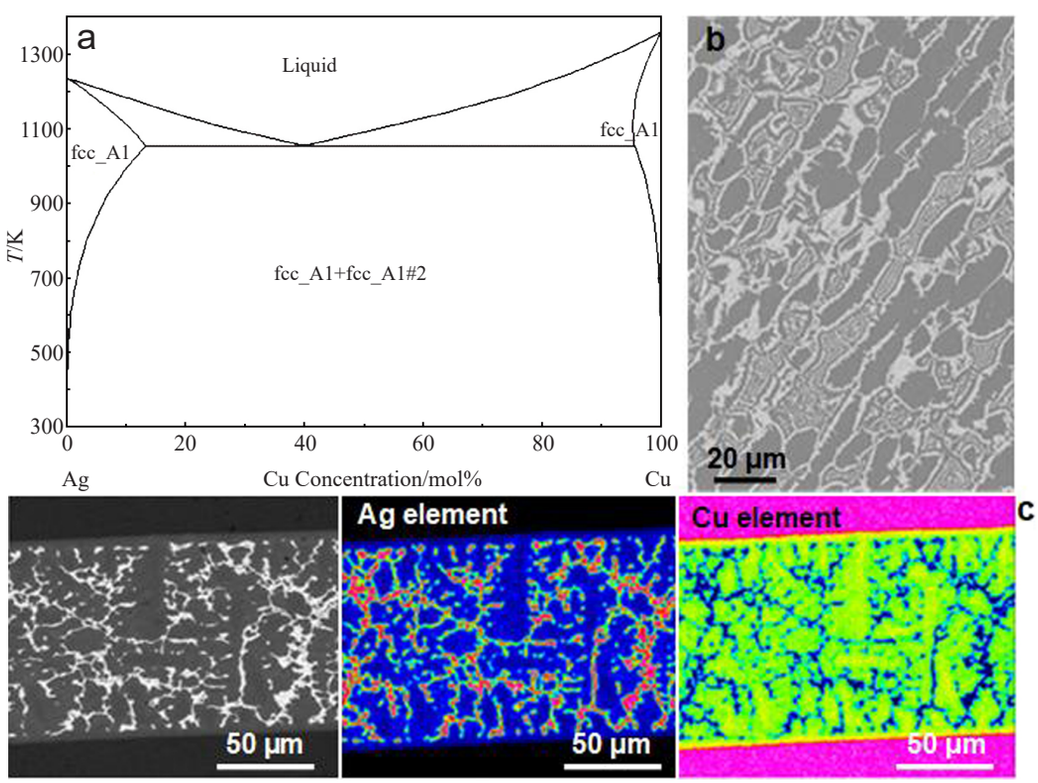

Fig.3 Ag-Cu binary phase diagram (a); microstructure in the BAg30CuZnSn brazing filler metal (b); cross-sectional microstructure and elements distribution in the Cu/BAg30CuZnSn/Cu joint (c)[26]

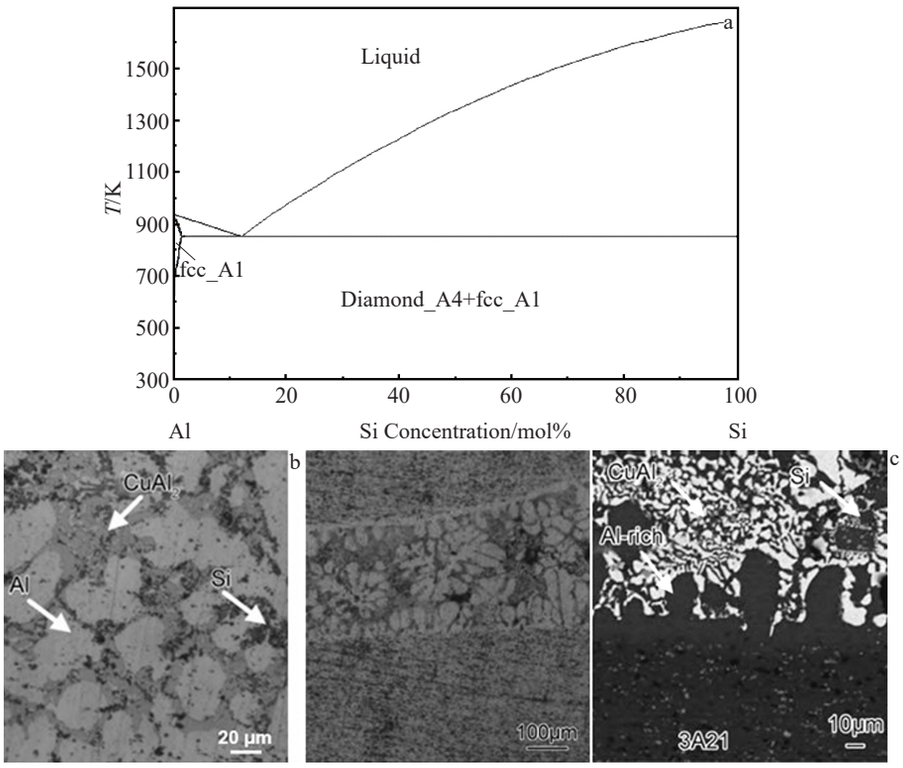

Fig.4 Al-Si binary phase diagram (a); microstructure in the Al-Si-Cu brazing filler metals (b); cross-sectional microstructure in the brazed joint and local magnification (c)[27]

dendrites, Si phases, and Al_2Cu IMCs, as shown in Fig. 4b. The Al and Si elements were the primary and secondary major elements, respectively, contributing to the high wettability of filler metals. The Al phase was formed at the Al-Si-Cu/3A21 joints (Fig. 4c), indicating a good metallurgical compatibility between filler metals and base materials.

The alloy formed by the primary element of the brazing filler metal has a melting temperature range lower than the solidus line of the material to be welded, which strictly avoids overheating of base materials during brazing. The primary and secondary elements in the brazing alloy system act as the "foundation and modifier", determining the fundamental properties of the brazing filler metals. Elements present in the third and fourth highest proportions typically serve as auxiliary components to modulate wettability and mechanical performance, primarily adjusting the melting temperature and flow-spreading property.

Trace elements in brazing alloys often play critical roles. For instance, Ti in AgCuSnTi[28], Li in AgCuLi[29], P in CuZnP[30], and Mg in AlSiMg[31] enhance the alloys' activity, while Sb in SnPb systems improves the mechanical properties of joints[32].

2.2 Determination principle of element composition ratio for spreadability

The spreadability of brazing filler metals refers to its spreading properties, gap-filling capability, and brazing processability which are essential for large-area or elongated brazing seams. The primary factor influencing spreadability is the liquid-to-solid phase ratios during brazing. As the brazing process involves dynamic temperature escalation, the proportion of liquid phase increases with increasing the temperature, consequently enhancing the spreadability of brazing filler metals.

Evidently, a smaller temperature difference between the liquidus and solidus lines of brazing filler metals represents a better fluidity, which explains the industry's preference for eutectic or near-eutectic brazing filler metals. In the design of filler metals, near-binary eutectic composition, such as BAl88Si[33], BAg72Cu[34], BNi89P[35], BSn63Pb[36], BZn98Al[37], and near-ternary eutectic composition, like BAl67CuSi[38], BCu76AgP[39], BNi76Cr14P10[40], are commonly selected.

When designing ternary, quaternary, or higher-order alloy brazing filler metals, the proportional relationships of primary elements can be determined through phase diagram analysis. Alternatively, coordinated adjustments can be made by preserving the elemental ratios of binary alloy eutectic points, that is, using the eutectic ratio between two primary elements as a foundational combination and then fine-tuning the proportions between these base combinations.

2.3 Mechanism of a third element addition for strength of brazing filler metals

The strength of brazing filler metal and the strength of brazed joints correspond to two distinct evaluation parameters. To enhance the versatility of brazing filler metals, it is generally necessary to improve the strength of filler

metals, though the strength of brazed joints remains the more critical factor in practical applications.

Alloys composed of two or three primary elements in brazing filler metals enhance mechanical properties through solid solution strengthening. However, achieving a balance between strength and toughness in near-eutectic alloys is challenging. This issue can be addressed by adding a third or fourth element to introduce the second-phase precipitation strengthening. Examples include systems such as AgCuNi[41], AgCuSn[42], CuZnSi[43], SnAgCu[44], SnPbAg[45], and ZnAlCu[46]. According to the origin of second phase, second-phase strengthening includes phase transformation strengthening, precipitation strengthening, and dispersion strengthening. Among them, phase transformation strengthening involves the formation of distinct microstructures through phase transformations induced by heat treatment and deformation; precipitation strengthening is achieved via solid solution and aging treatments to precipitate fine, dispersed, and uniformly distributed second-phase particles; dispersion strengthening introduces hard, finely dispersed, and uniformly distributed second-phase particles to form a composite structure through powder metallurgy, ion implantation, or chemical infiltration.

Another approach to strengthen the brazing filler metals is grain refinement strengthening, achieved by incorporating high-melting-point elements or grain refiners. For instance, trace amounts of Cr, Ti, or Zr elements are added to Ag based or Cu based filler metals[47–48], and Ti, B, Sr, Sc, or Zr elements are introduced to Al based filler metals[49]. Additionally, grain refinement in brazing filler metals can be achieved through rapid cooling during liquid-solid transformation, cold deformation, hot deformation, weld seam area treatment, recrystallization, as well as compound processes.

2.4 Design of trace elements for enhanced strength of brazed joints

It is noteworthy that improving the strength of brazed joints through reactions between filler metals and base materials during brazing represents an advanced design strategy of filler metals. This involves introducing trace elements capable of strongly interacting with the base materials. Besides the solid solution strengthening, other mechanisms for strengthening brazed joints include second-phase strengthening through phase transformation, precipitation, segregation, or dispersion, as well as grain refinement and deformation strengthening. All four alloy strengthening mechanisms are applicable in brazing technology, and the reaction between filler metals and base materials is considered during design. This involves the dissolution of base materials into filler metals and the simultaneous diffusion of filler metals components into base materials, utilizing elements from base materials as sources for strengthening phases. Representative examples include Ni based brazing filler metals for joining stainless steel, Zn based brazing filler metals for brazing aluminum, and Sn based solders for Cu soldering.

A specialized category involves filler metals incorporating small amounts of active elements for brazing difficult-to-weld materials. The active elements refer to the elements that react intensely with the base materials, such as Ti and Zr elements added in AgCu alloys for ceramic brazing[50], trace Ga element doped in AlSiZnAg filler metals for aluminum joining[51], and B element contained in NiCrSi filler metals for superalloy brazing[52].

2.5 Design of special brazing filler metals for physico-chemical properties

For enhancing electrical conductivity, the design of filler metals should prioritize single-element or binary alloys with face-centered cubic (fcc) structures, such as Ag, Cu, Al, and AgCu systems. To improve corrosion resistance, design considerations must include elemental electronegativity, electrode potential, and the density of formed compound films. For instance, adding Ni and Sn to Ag based brazing filler metals enhances corrosion resistance[53], while excluding Cu and Zn from Al based brazing filler metals also improves corrosion resistance[54].

In neutron irradiation environments, boron (B) exhibits a dual effect. Due to the effective neutron absorption capability, B is either restricted or intentionally used in large quantities. Similarly, Ag element has special requirements in nuclear engineering.

2.6 Composition design for processability of brazing filler metals

Brazing filler metals are commonly manufactured in diverse forms, including plates, strips, foils, sheets, wires, rods, threads, rings, powders, and pastes. The processing methods of filler metals encompass melting, casting, powder spraying, powder reduction, granulation, extrusion, rolling, drawing, straightening, ring forming, and amorphization. Among them, the feasibility of melting, casting, granulation, microsphere production, rolling, and drawing is closely related to the composition of brazing filler metals.

For the cold forming of filler metals, the plasticity of filler metals determines the feasibility and efficiency of processing. The design principle involves analyzing binary phase diagrams to determine the maximum solid solubility of secondary elements in the primary matrix at ambient temperatures. For instance, when the Zn content in Cu-Zn systems is low and Zn/Cu ratio≤39: 61, α-phase is formed, enabling the effective cold rolling/drawing. When the Zn content is relatively high and Zn/Cu ratio≥45: 55, β-phase is formed, significantly hindering the cold workability[55]. Therefore, when introducing a third element, careful attention should be paid to the solid solubility of added elements in both primary and secondary matrix components.

3 Experiment

The raw materials of Ag based brazing filler metals were pure Ag (99.99%), pure Cu (99.99%), pure Zn (99.99%), and pure Sn (99.99%). The raw materials were melted in an induction melting furnace, then poured into cast iron at 690 ℃ to produce ingots, and cooled rapidly. Then, the brazing alloys samples with desirable dimensions were cut from the ingot

using wire electrical discharge machining. For the Ti based brazing filler metals, pure Ti (99.99%), pure Zr (99.99%), pure Cu (99.99%), and pure Ni (99.99%) were melted in a vacuum arc melting furnace to prepare button ingots of brazing alloys. Then, the ingots were heated to 1000 ℃ and melted in an induction melting furnace, and the melt was ejected onto the surface of a rotating copper roller to produce foil of Ti based amorphous brazing alloys with a cooling rate of about 106 ℃/s. The melting temperatures of Ag based and Ti based brazing filler metals were measured by an infrared radiation thermometer. The details of raw materials for preparing Al based, Cu based, and Ni based brazing filler metals were reported in our previous studies[48–49,52].

The liquidus and solidus temperatures of different brazing filler metals were measured through differential thermal analysis, and the samples were heated and cooled in argon protected atmosphere. To determine the wettability of brazing filler metals, the square samples were placed on the surface of base materials, heated to the set temperature, and held for a certain time. The spreading areas were measured 3 times for each sample to obtain the average value.

The Cu/BAg55ZnCuSn/Cu joints were brazed using BAg55ZnCuSn brazing filler metals in an induction heating furnace. The brazing of Ti alloys using TiZrCuNi amorphous brazing filler metals was conducted in a vacuum brazing furnace. The detailed information of brazing experiments using Al based, Cu based, and Ni based brazing filler metals was reported in our previous studies[48–49,52].

The tensile and shear strengths of brazing filler metals and joints were determined using a universal electron materials tester at room temperature. The microstructures of brazing filler metals, cross-sectional microstructures, and fracture morphologies of brazed joints were detected by Phenom Pro-XL scanning electronic microscope equipped with an energy dispersive spectrometer (EDS).

4 Application of Design Guidelines and Results Discussion

4.1 Examples for design of typical brazing filler metals

4.1.1 BAg55ZnCuSn brazing filler metals

To meet the requirements of wettability and mechanical properties of Ag based brazing filler metals and brazed joints for the hard windings and end-rings of large generator rotors, the BAg55ZnCuSn brazing filler metals were developed, as illustrated in Fig. 5. The chemical composition of BAg55ZnCuSn brazing filler metals determined by EDS is within the following ranges: 54.0wt%–56.0wt% Ag, 20.0wt%–22.0wt% Cu, 20.0wt%–24.0wt% Zn, and 1.5wt%–2.5wt% Sn. The microstructures of cast BAg55ZnCuSn brazing filler metals consist of Ag-rich phase, eutectic structures, and IMCs (Fig. 5a), while the microstructures in brazed joints contain Cu-rich phase, Ag-rich phase, eutectic structures, and IMCs (Fig. 5b). The primary and secondary major elements in BAg55ZnCuSn brazing filler metals were Ag and Zn, respectively, which exhibit metallurgical compatibility with the Cu based materials. The solidus and liquidus temperatures were 642 and 663 ℃, respectively, and the spreading area of liquid BAg55ZnCuSn on the surface of Cu base materials was 245 mm^2. The tensile strength, elongation, and impact work of BAg55ZnCuSn brazing filler metals were 479.4 MPa, 13.9%, and 64.9 J, respectively, and the tensile strength and impact work of Cu/BAg55ZnCuSn/Cu joints were 228.7 MPa and 56.2 J, respectively, as shown in Fig. 5c. The wettability of brazing filler metals is attributed to the decreased melting temperature after addition of Cu and Sn elements, while the strength improvement of brazing filler metals and joints is ascribed to the solid solution strengthening and secondary-phase strengthening. Additionally, the good corrosion resistance of the Cu/BAg55ZnCuSn/Cu joints is related to the addition of Sn element, elevating the electrode potential. In comparison to BAg56CuZnSn, the Sn content in BAg55 ZnCuSn is reduced from 4.5%–5.5% to 1.5%–2.5%, resulting in a significant improvement in workability. Meanwhile, the silver content in BAg55ZnCuSn is reduced by 1%, providing a certain cost advantage.

4.1.2 AlMgMnCrTiLa brazing filler metals

To obtain high-performance and clean Al based brazing filler metals, Lu et al[49] developed an Al5Mg0.1Mn0.1Cr0.1Ti-0.45La multicomponent brazing alloy. The microstructure was mainly composed of an α-Al matrix, Al_3Mg_2 phase, $Al_{11}La_3$ phase, and a small amount of impurity phase, as shown in Fig. 6a. Ti and B elements promoted the nucleation of α-Al and refined the grains of Al dendrites (Fig.6b). Meanwhile, La element enhanced the constitutional supercooling at the front of liquid/solid interface, refining the grains and reducing its dimensions. This brazing alloy after Sc addition with different contents exhibited high tensile strength, elongation, and impact energy, and a ductile fracture morphology was observed on the fracture surface, as shown in Fig. 6d. The enhanced strength was attributed to the solid solution strengthening, grain refinement strengthening, and second-phase strengthening, promoting the application of this brazing alloys in brazing Al alloy components for rail transit. These filler metals were mainly prepared through processes such as smelting, casting, extrusion, and drawing. It has a low content of alloying elements and low brittleness, and it is easy to process. There are no precious metal elements in the filler metals, and the content of rare earth elements is extremely low, reflecting a lower cost.

4.1.3 TiZrCuNi amorphous brazing filler metals

Addressing the challenges of low strength of Ti alloys joints and suboptimal composition design of Ti based brazing filler metals, Zhengzhou Research Institute of Mechanical Engineering Co., Ltd developed an amorphous foil filler metal with low melting temperature, as shown in Fig. 7a. The chemical composition of amorphous filler metals is Ti27.6Zr22.4Cu39Ni11, and the structure of filler metals is determined to be amorphous through X-ray diffractometer (XRD) analysis in Fig. 7b. The spreading area is 55.6 mm^2, and the melting temperature is 895.5 ℃. Ti solute solutions and Ti-Cu IMCs are formed at the interface between filler

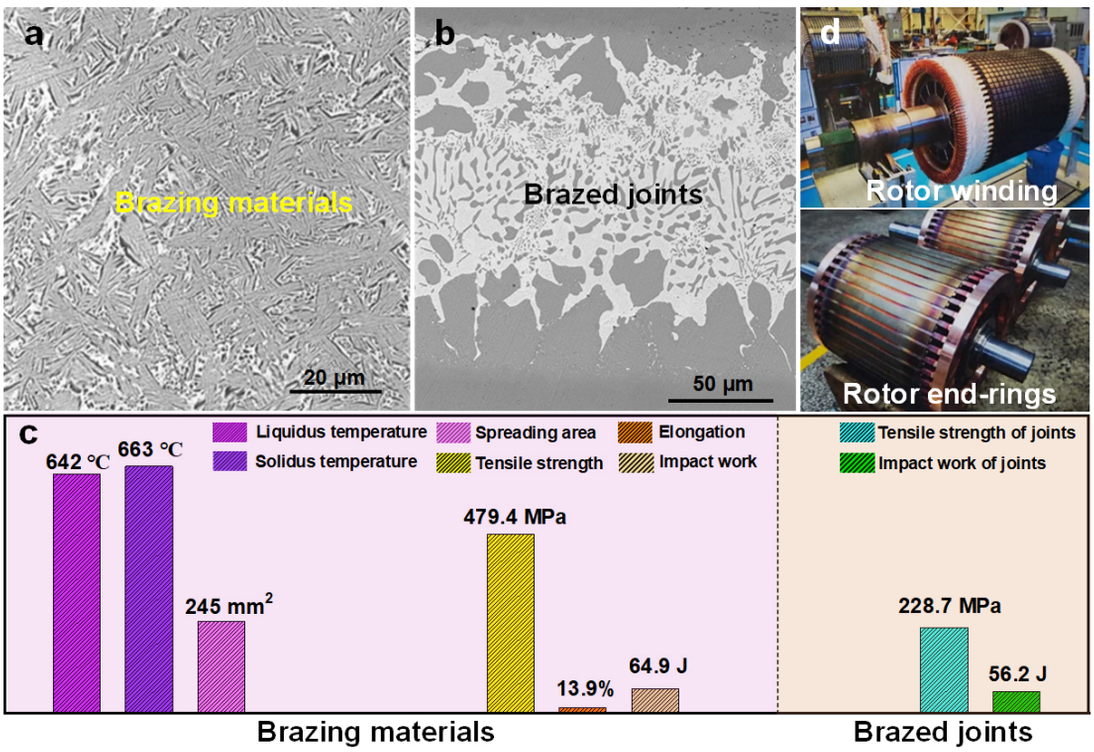

Fig.5 Microstructures (a–b) and properties (c) of BAg55ZnCuSn brazing materials and brazed joints; application of large generator in rotors (d)

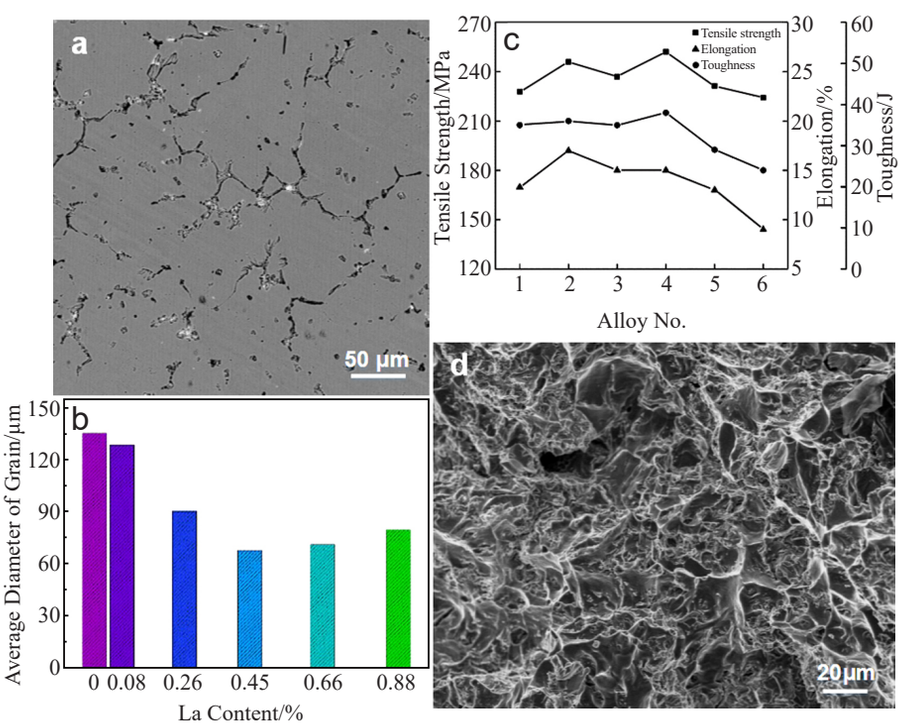

Fig.6 Microstructure (a), grain size (b), mechanical properties (c), and fracture morphology (d) of Al5Mg0.1Mn0.1Cr0.1Ti0.45La brazing filler metals[49]

metals and TC4 alloys (Fig. 7c), and the shear strength of brazed joints is 235.6 MPa, as illustrated in Fig. 7d. The amorphous foil filler metals have been successfully utilized to braze Ti alloys heat exchangers (Fig.7e). The high strength of brazed joints is attributed to the solid solution strengthening through the solid solution of Zr and Ni elements in Ti alloys and the interfacial Ti-Cu IMCs through the enhanced reaction between amorphous filler metals and base materials. This brazing filler metal features amorphous ribbon forms in one step, without the need for rolling, annealing, or other

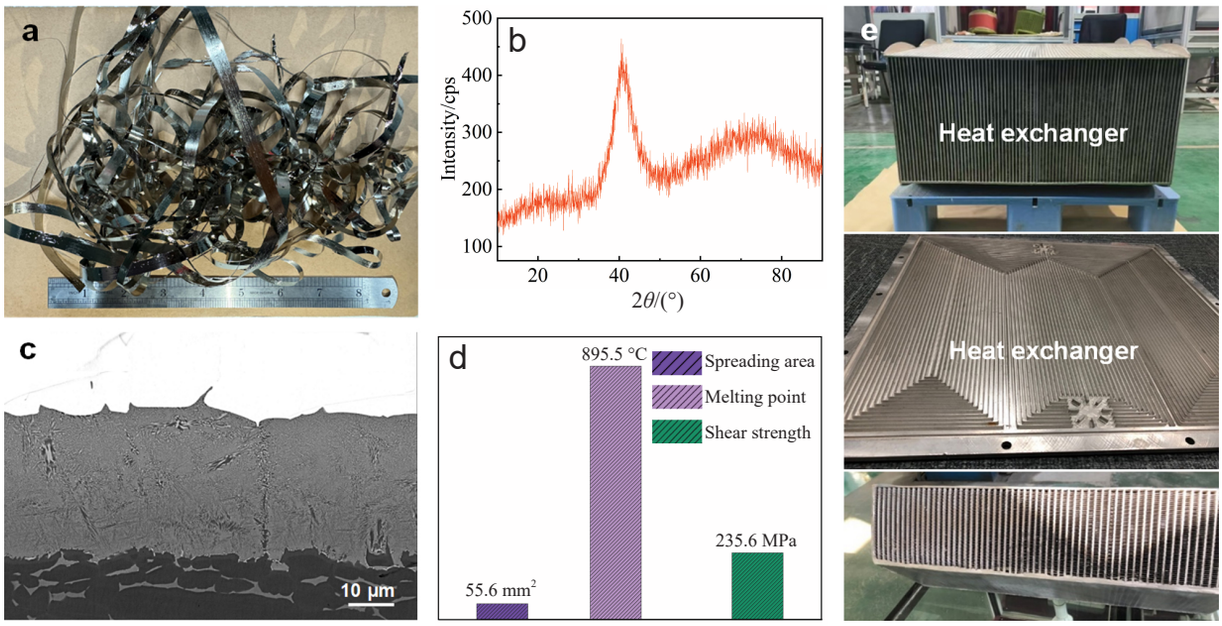

Fig.7 Macrostructure (a) and XRD pattern (b) of TiZrCuNi amorphous brazing filler metals; microstructure (c) and properties (d) of amorphous brazing filler metals and filler metals/TC4 brazed joints; application in heat exchanger (e)

processes, resulting in a relatively low manufacturing cost.

4.1.4 CuSnTi brazing filler metals

To obtain high-performance cutting tools, Zhao et al[48] fabricated a Cu70Sn20Ti10 brazing filler metals using in-situ synthesis method, forming a reliable polycrystalline cubic boron nitride (PcBN)/YG8 cemented carbide joints. The microstructures of CuSnTi filler metals consisted of Cu-rich phase, Cu-Sn IMCs, and eutectic structures, as shown in Fig.8a. The filler metals enabled an effective joining between PcBN and YG8 cemented carbide with an average shear strength of 96.06 MPa. The fracture behavior occurred at the PcBN side, and no separation between filler metals and base

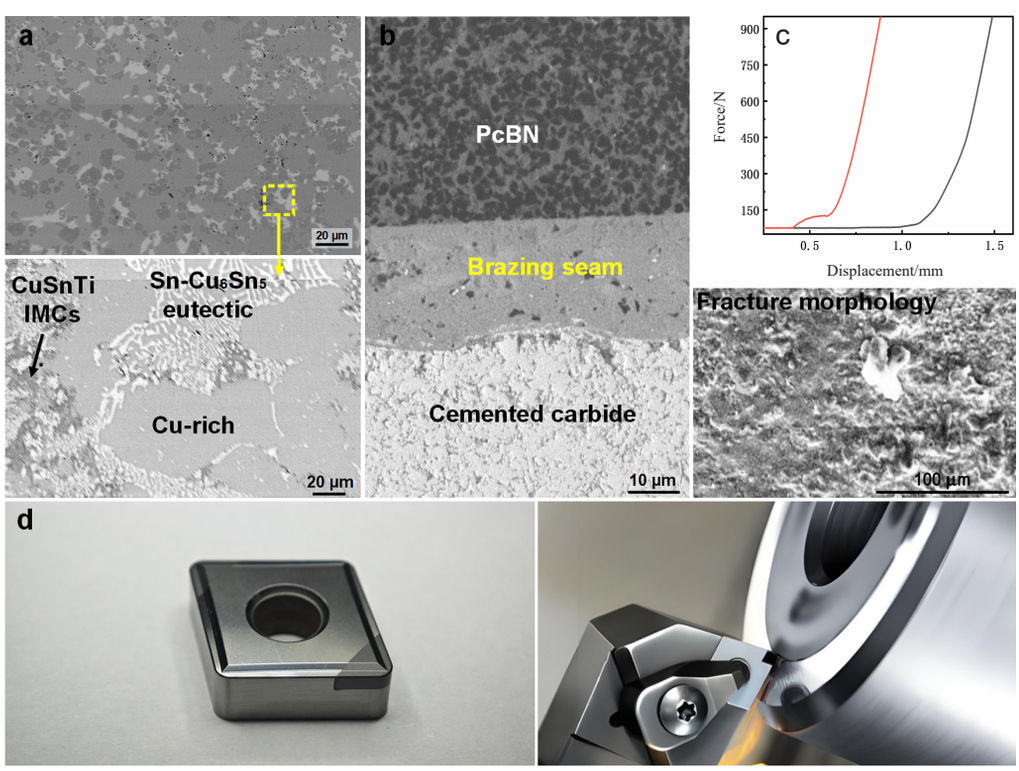

Fig.8 Microstructure of Cu70Sn20Ti10 brazing filler metals (a); cross-sectional microstructure of the PcBN/cemented carbide brazed joint (b); properties and fracture morphology of brazed joints (c); application in cutting tools for CNC machine tools (d)[48]

materials was found, indicating good strength and toughness of the brazed joints (Fig. 8b – 8c). The addition of active Ti elements strengthened the reaction between Cu based filler metals and base materials including PcBN and YG8 cemented carbide, ensuring metallurgical bonding and wide application in the manufacture of cutting cools for computer numerical control (CNC) machine tools (Fig. 8d). The CuSnTi brazing filler material was produced through vacuum melting and gas atomization to form a powdery filler, and its price was substantially lower than that of Ag based active brazing filler metals, demonstrating a significant cost advantage.

4.1.5 NiCrSiBFe brazing filler metals

The brazing filler metals for joining diamond and steel substrate should possess both excellent wettability to form a metallurgical bonding and sufficient wear resistance to match the abrasive resistance of hard particles in the coatings. Zhengzhou Research Institute of Mechanical Engineering Co., Ltd[52] developed a Ni82Cr7Si4.5B3.1Fe3 brazing filler metal, as shown in Fig. 9a. The Cr element in the filler metals can significantly improve the metallurgical reaction between the diamond and 65Mn steel. A reaction layer was formed between filler metals and steels (Fig. 9b), which was a layered solid solution phase formed through interdiffusion between Fe and Ni atoms. The addition of TiC particles reduced the wear of the coatings and decreased the mass loss of the coatings, as shown in Fig. 9c. In addition, the addition of B and Si elements reduced the melting point of Ni based brazing filler metals, minimizing thermal damage of diamond and enhancing the wear resistance of diamond brazed screw conveyor and rotary tiller blades (Fig. 9d). The NiCrSiBFe brazing filler metals contained brittle and hard phases, making it difficult to be fabricated into sheet, wire, or ribbon forms. It is usually produced by vacuum gas atomization to form a powdery material. The matrix element is Ni, and its price is significantly lower than that of Ag, providing a cost advantage.

4.2 Morphological evolution and growth mechanism of typical microstructures

For the Ag based filler metals after compositional design, the microstructures in the filler metals mainly consist of the Ag-rich phase, Cu-rich phase, eutectic structures, and diversified IMCs[56]. The dimension, morphology, and distribution of various phases have an important influence on the physical and mechanical properties of filler metals and brazed joints. Particularly, the eutectic structure, including the Ag-Cu binary eutectic and Ag-Cu-β ternary eutectic structures, is one of the typical microstructures in the Ag based filler metals[57]. Based on the results from the previous studies, it has been reported that the difference in additional alloying elements (category[58] and content[59]), controlled solidification conditions (temperature[60] and solidification velocity[61]), and external energy field (electric field[62], magnetic field[63], and ultrasonic field[64]) can promote the formation of eutectic structures with various morphologies, such as Al-Si[65] and Sn-Cu_6Sn_5[66] binary eutectic structures as well as Al-Si-Al_2Cu[67] and Sn-Cu_6Sn_5-Ag_3Sn[68] ternary eutectic structures. It is worth noting that the Al-Si binary eutectic consists of a non-faceted Al phase and a faceted Si phase, while the Sn-Cu_6Sn_5 binary eutectic comprises a non-faceted Sn phase and a faceted Cu6Sn5 phase. However, the Ag-Cu binary eutectic is composed of both non-faceted Ag and non-faceted Cu phases. For the Ag based filler metals, the trace alloying elements, including Zn,

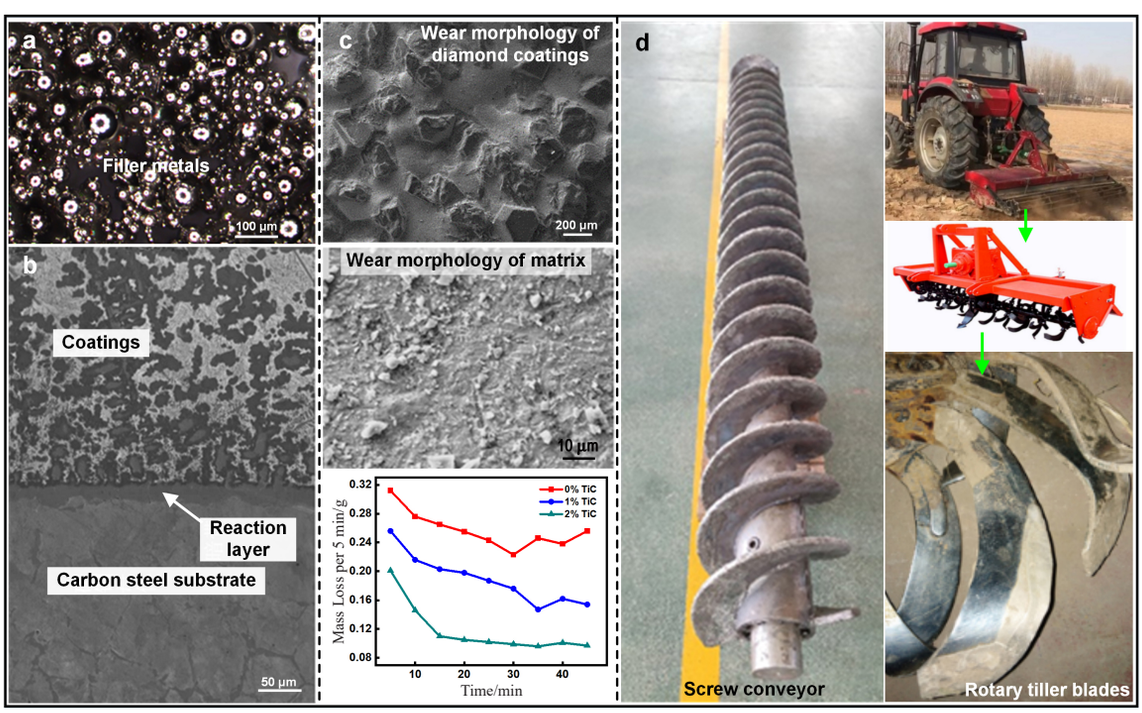

Fig.9 Microstructures of Ni based brazing filler metals (a) and diamond coatings (b); wear morphologies of diamond coatings and matrix and mass loss of diamond coatings (c); application in diamond brazed screw conveyor and rotary tiller blades (d)[52]

Sn, Ni, Cd, In, and Mn elements, are selectively added to prepare BAg72Cu, BAg70CuZn, BAg60CuSn, BAg60 CuZnSn, BAg50CuZnCd, BAg40CuZnIn, BAg54CuZnNi, BAg63CuSnNi, and BAg27CuZnMnNi filler metals with desirable properties. The microstructures of these filler metals mainly consist of white Ag-rich phase, black Cu-rich phase, and interlaced white/black eutectic structures, as illustrated in Fig. 10. The Ag-Cu binary eutectic and Ag-Cu-β ternary eutectic structures with different morphologies are always formed in the filler metals. Therefore, uncovering the effect of alloying elements on the growth behavior and morphological evolution of the binary and ternary eutectic structures is a key to control the micro-structures and properties of the filler metals and brazing seam.

4.2.1 Ag-Cu binary eutectic structures

For the BAg72Cu, BAg72CuLi, BAg70CuZn, BAg56CuNi, and BAg60CuSn filler metals, the regularly formed lamellar, fibrous, and anomalous Ag-Cu binary eutectic structure contains two phases: Ag-rich phase and Cu-rich phase[69]. Ding et al[70] found that increasing the Sn content and solidification velocity promoted the transformation from lamellar Ag-Cu binary eutectic structure to fibrous and anomalous eutectic structures. Qin et al[71–72] controlled the sub-rapid cooling rates to investigate the effect of cooling rate on the Ag-Cu binary eutectic structures. The increasing cooling rate resulted in the morphological transition from eutectic dendrites to equiaxed eutectic colony and spherical eutectic colony, accompanied by the primary phase selection and changed eutectic lamellar spacing. After addition of Sb alloying element, the solidification interface of Ag-Cu eutectic structures changed from a cellular morphology into a cellular dendrite and an undeveloped dendrite, and the tip radius decreased. Therefore, the addition of the third component strongly affects the dimension and morphology of Ag-Cu binary eutectic structure. However, the morphological transition and growth mechanisms of Ag-Cu binary eutectic structures in the Ag based filler metals versus the addition contents of the third components (Zn, Ni and Mn) remain unclear.

Fig. 11 shows the microstructures of Ag based filler metals after addition of Zn, Ni, and Mn alloying elements. The Ag-Cu binary eutectic structures have the lamellar, fibrous, and anomalous morphologies. The fraction of lamellar eutectic structures (LESs) is larger than that of fibrous eutectic structures (FESs) and anomalous eutectic structures (AESs). The AES is mostly located at the junction of LES clusters and/or FES clusters. With increasing the Zn addition, the fraction of FES and AES increases, as shown in Fig. 11a – 11c. When the content of Ni and/or Mn addition increases, the eutectic structures are transformed from LES to FES and AES, as illustrated in Fig. 11d – 11i. To uncover the formation and morphological transition mechanisms, the growth mechanisms of LES, FES, and AES will be analyzed.

There is a competition between Ag-Cu lamellar eutectic

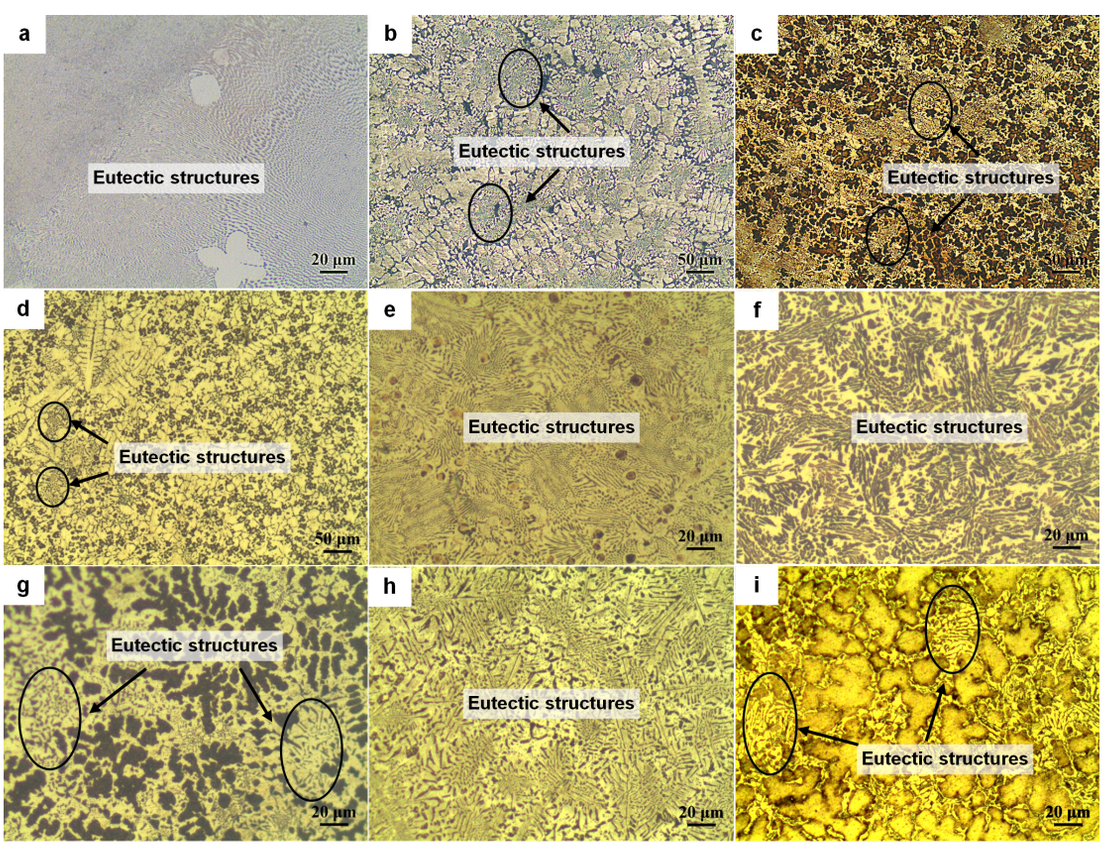

Fig.10 Microstructures of different Ag based brazing filler metals: (a) BAg72Cu, (b) BAg70CuZn, (c) BAg60CuSn, (d) BAg60CuZnSn, (e) BAg50CuZnCd, (f) BAg40CuZnIn, (g) BAg54CuZnNi, (h) BAg63CuSnNi, and (i) BAg27CuZnMnNi

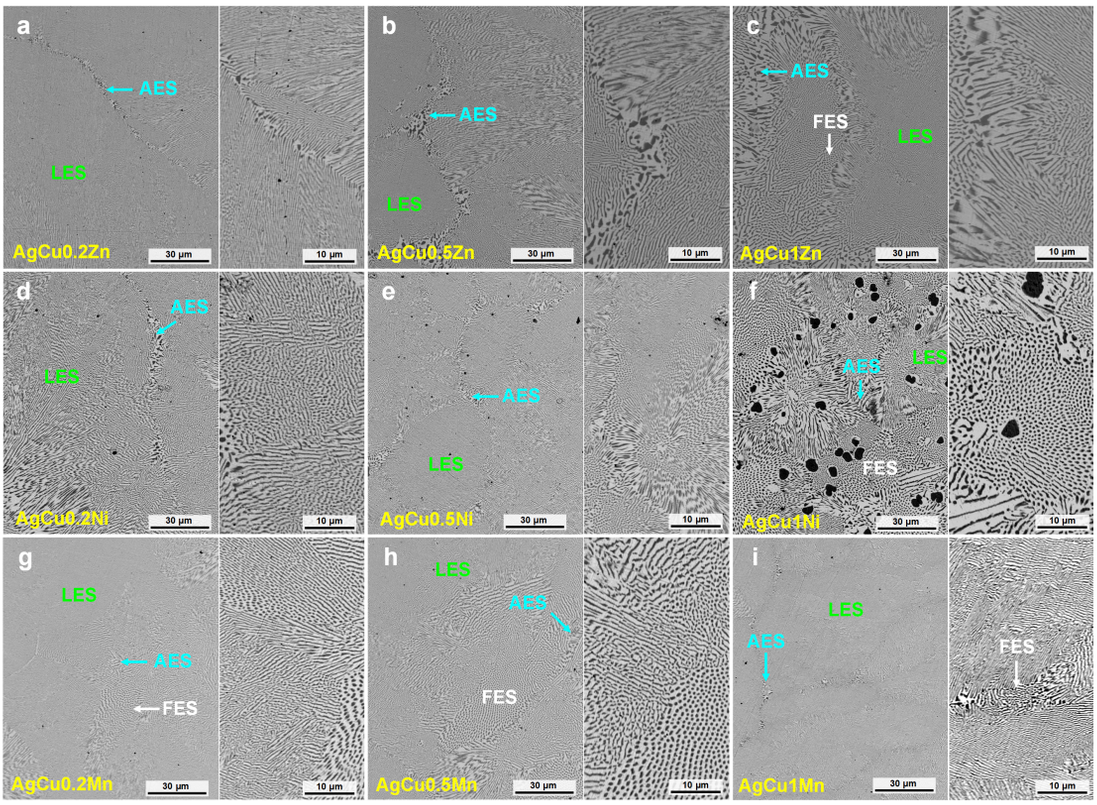

Fig.11 Microstructures and magnification of Ag-Cu binary eutectic structures after addition of Zn (a–c), Ni (d–f), and Mn (g–i) alloying elements with different contents

structures and Ag-Cu fibrous eutectic structures, following the growth model established by Jackson et al[73]. This is attributed to the addition of Zn, Ni, and Mn elements which change the undercooling of Ag based brazing filler metals during solidification, accompanied by the changes in the lamellar spacing. As the growth undercooling and spacing of Ag-Cu LES satisfied the critical values, the Ag-Cu eutectic structures are transformed from LES to FES. Fig. 12 shows the morphology and schematic diagram of lamellar Ag-Cu eutectic structures. The lamellar Ag-Cu eutectic structures consist of regular alternation of coupled Ag lamellae and Cu lamellae, as shown in Fig.12a. The relationship curve of solute changes at the liquid/solid (L/S) interface front of eutectic structure growth and corresponding Ag-Cu binary phase diagram are shown in Fig. 12b. To describe the composition distribution (C_{Cu}) in the molten brazing filler metals at the L/S front, assuming the eutectic phases growth in a stable state and constant growth rate (v), the solute distribution within the boundary layer can be described using two-dimensional spatial coordinates[74]:

$$\nabla^2 C_{Cu} + \frac{v}{D_L^{Cu}}\frac{\partial C_{Cu}}{\partial z} = \frac{\partial^2 C_{Cu}}{\partial x^2} + \frac{\partial^2 C_{Cu}}{\partial z^2} + \frac{v}{D_L^{Cu}}\frac{\partial C_{Cu}}{\partial z} = 0 \quad (1)$$

where x is the distance in the lateral growth direction of Ag-Cu eutectic structures, with the Ag phase as the origin; z is the distance to L/S interface; C_{Cu} is solute composition of Cu atoms at a specific position at the front of L/S interface; v is the growth rate of the Ag-Cu eutectic interface; D_L^{Cu} is the diffusion coefficient of Cu atoms in the molten Ag based brazing filler metals. Solving Eq.(1) yields the distribution of Cu solute atoms at the L/S interface front of Ag-Cu eutectic growth[75]:

$$C_{Cu}(x,z) = C_{Cu}^0 + A_0 \exp\left(-\frac{v}{D_L^{Cu}}z\right) + \sum_{i=1}^{\infty}\left[A_i \cos\left(\frac{2i\pi x}{d}\right)\exp\left(-\frac{2i\pi}{d}z\right)\right] \quad (2)$$

$$A_0 = -\left(\Delta C_{Cu}^{Ag\ phase} f_{Ag\ phase} + \Delta C_{Cu}^{Cu\ phase} f_{Cu\ phase}\right) \quad (3)$$

$$A_i = -\frac{vd}{D_L^{Cu}\pi^2}\left(\Delta C_{Cu}^{Ag\ phase} - \Delta C_{Cu}^{Cu\ phase}\right)\frac{\sin\left(i\pi f_{Ag\ phase}\right)}{i^2} \quad (4)$$

where C_{Cu}^0 is the solute concentration of Cu atoms in the melt of filler metals far from the L/S interface front of Ag-Cu eutectic growth; $\Delta C_{Cu}^{Ag\ phase}$ and $\Delta C_{Cu}^{Cu\ phase}$ are the concentration gradients of Cu atoms at the L/S interface front in the Ag phase and Cu phase of Ag-Cu eutectic structures, respectively; $f_{Ag\ phase}$ and $f_{Cu\ phase}$ are the molar fractions of the Ag phase and Cu phase in the eutectic structure, respectively; d is the eutectic lamellar spacing (d=$2l_{Ag}$+$2l_{Cu}$). When the difference ($\Delta C_{Cu}^{Ag\ phase} - \Delta C_{Cu}^{Cu\ phase}$), growth rate ($v$), and lamellar spacing (d) increase, the concentration difference of solute atoms at the growth fronts of Ag phase and Cu phase becomes larger. If the Cu solute elements do not diffuse timely and the lateral diffusion distance is relatively large, the enrichment of Cu element occurs at the L/S interface front of Ag-Cu eutectic structures. Subsequently, the lamellar eutectic will become unstable, and will be transformed to eutectic structures with

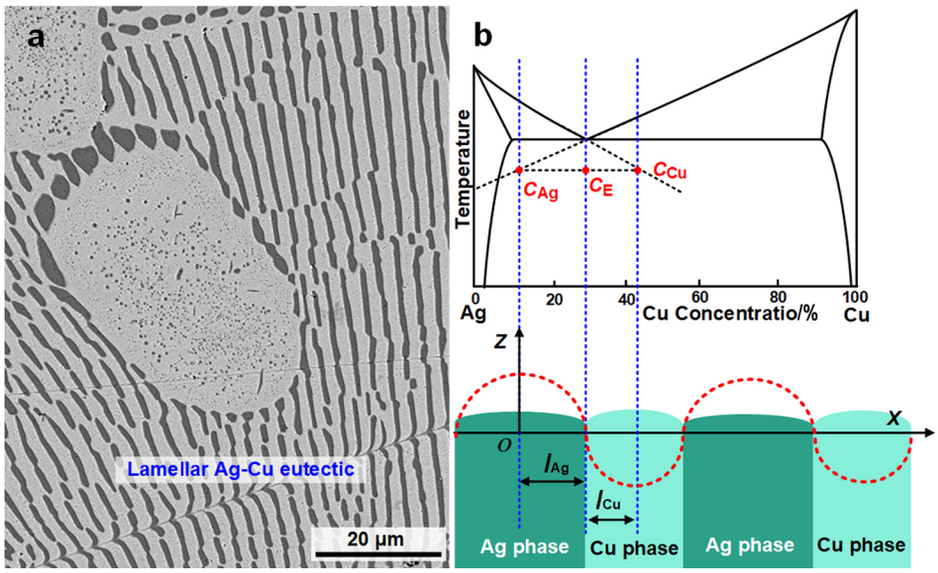

Fig.12 Morphology (a) and schematic diagram (b) of lamellar Ag-Cu eutectic structures

other different morphologies.

Fig. 13 shows the morphology and schematic diagram of fibrous Ag-Cu eutectic structures. The fibrous Ag-Cu eutectic structures in 3D contain rod-like Cu phases, and round Cu phases are uniformly distributed in Ag matrix, as shown in Fig. 13a. The Ag-Cu binary alloy system with Ag and Cu elements has equilibrium eutectic temperature (T_E) and eutectic concentration (C_E), as shown in Fig. 13b. The ΔC_{Ag} and ΔC_{Cu} are the concentration differences between Ag phase, Cu phase and eutectic point (T_E, C_E). The radius of rod-like Cu phase is λ_{Cu}, and the Ag phase is the matrix. Following the classical Jackson and Hunt model[76], the steady-state solute diffusion profile in the cylindrical system can be expressed by Eq.(5).

$$\left(\frac{\partial^2 C}{\partial \lambda^2}+\frac{1}{\lambda}\frac{\partial C}{\partial \lambda}\right)+\left(1-\frac{V^2}{V_D^2}\right)\frac{\partial^2 C}{\partial Z^2}+\frac{V}{D}\frac{\partial C}{\partial Z}=0 \tag{5}$$

The solution of the diffusion in Eq.(5) is obtained:

$$C=\begin{cases}C_\infty+A_0\exp\left[-\dfrac{V_Z}{D\left(1-V^2/V_D^2\right)}\right]+\sum_{n=1}^{\infty}A_n J_0\left(\dfrac{\gamma_n r}{R}\right)\exp\left(-\omega_n Z\right), & V<V_D\\ C_\infty, & V\geqslant V_D\end{cases} \tag{6}$$

$$\omega_n=\frac{V}{2D\left(1-V^2/V_D^2\right)}+\left\{\left[\frac{V}{2D\left(1-V^2/V_D^2\right)}\right]^2+\left(\frac{\gamma_n}{R}\right)^2\right\}^{1/2} \tag{7}$$

where C_∞ is the composition in the liquid brazing filler metals far from the interface; A_0 and A_n are the Fourier coefficients; J_0 is the Bessel function of zero order; γ_n is the n-th Bessel function of first order. The values of A_0 and A_n can be determined based on the solute conservation at the L/S interface. For the Ag-Cu binary phase diagram, the liquidus and solidus lines below T_E are not parallel. The concentration of Cu phase in the solid (C_{SCu}) increases with C_E, while the concentration of Ag phase in the solid (C_{SAg}) increases with $(1-C_E)$. A_0 and A_n can be expressed by Eq.(8–9), respectively.

$$A_0=\frac{(1-k)}{k}\frac{C_\infty\lambda_{Cu}^2-\left(1-C_\infty\right)\left[\left(\lambda_{Cu}+\lambda_{Ag}\right)^2-\lambda_{Cu}^2\right]}{\left(\lambda_{Cu}+\lambda_{Ag}\right)^2} \tag{8}$$

$$A_n=4\sqrt{f_\alpha}(1-k)\frac{J_1\left[\gamma_n\left(\lambda_{Cu}/R\right)\right]}{\gamma_n\left[J_0\left(\gamma_n\right)\right]^2}\times\left\{\frac{1}{\sqrt{1+\left[p_n\left(1-V^2/V_D^2\right)\right]^2}-1+2k}\right\} \tag{9}$$

The average composition ($\overline{C_{Cu}}$ and $\overline{C_{Ag}}$) in the liquid Ag based brazing filler metals at the interface ahead of the Cu phase and Ag phase is obtained.

$$\overline{C_{Cu}}=C_\infty+A_0+\frac{4V\left(\lambda_{Cu}+\lambda_{Ag}\right)}{D}\Delta C_0 M \tag{10}$$

$$\overline{C_{Ag}}=C_\infty+A_0-\frac{4\lambda_{Cu}^2\left(\lambda_{Cu}+\lambda_{Ag}\right)}{\left(\lambda_{Cu}+\lambda_{Ag}\right)^2-\lambda_{Cu}^2}\frac{V\Delta C_0 M}{D} \tag{11}$$

$$M=\sum_{n=1}^{\infty}\frac{\left[J_1\left(\gamma_n\sqrt{f_\alpha}\right)\right]^2}{\gamma_n^3\left[J_0\left(\gamma_n\right)\right]^2}\left\{\frac{p_n}{\sqrt{1+\left[p_n\left(1-V^2/V_D^2\right)\right]^2}-1+2k}\right\} \tag{12}$$

Fig. 14 shows the morphologies of anomalous Ag-Cu eutectic structures, which is characteristic of irregular Cu phase distributed on the Ag matrix. The formation of anomalous Ag-Cu eutectic structures has two different formation mechanisms[77]. One is transition from a lamellar eutectic structure LES to an anomalous eutectic structure AES, as shown in Fig. 14a. During the rapid solidification of Ag based brazing filler metals, the release of latent heat leads to the remelting of LES. The solute trapping effect during solidification promotes the supersaturation of Cu atoms in the Cu-rich phase of LES, generating a Cu concentration gradient

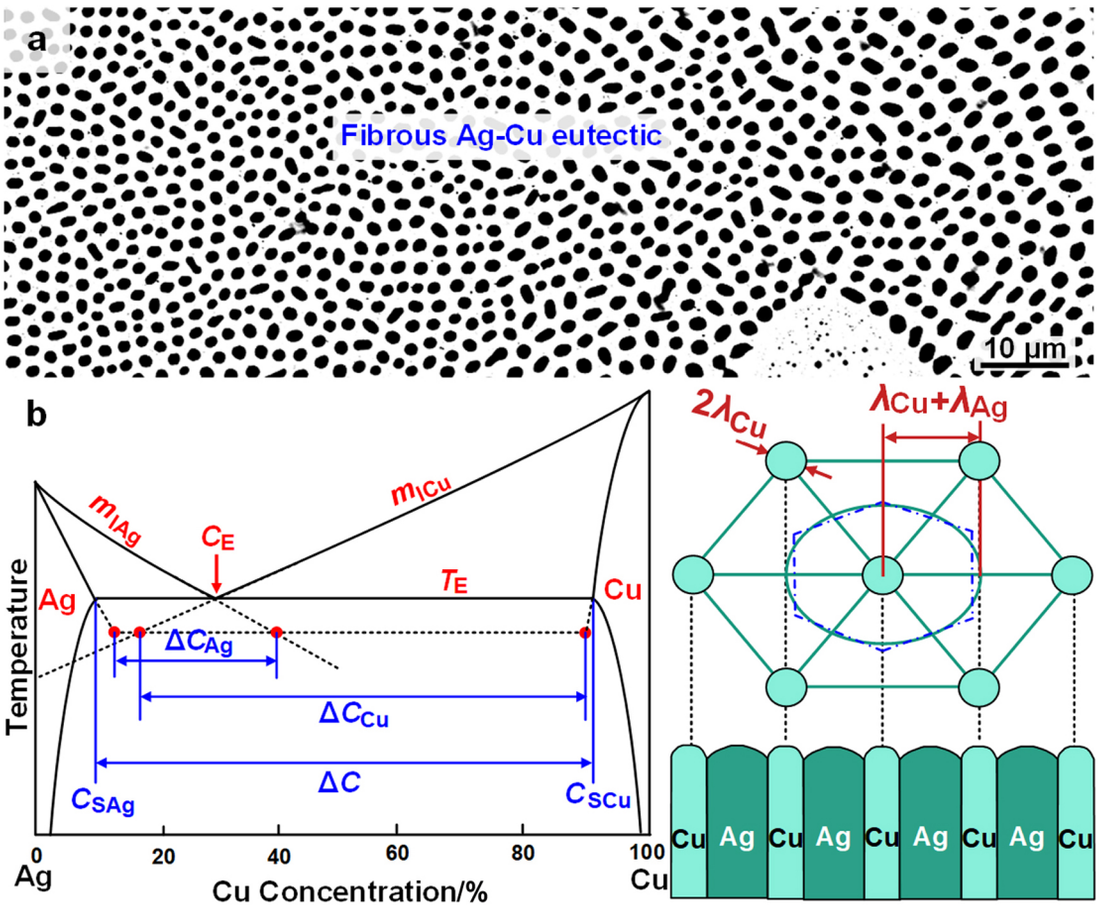

Fig.13 Morphology (a) and schematic diagram (b) of fibrous Ag-Cu eutectic structures

(ΔC). This gradient drives the diffusion of Cu solutes from low to high concentrations, enhancing the disturbance within Cu-rich phase. The combination of concentration gradients and curvature differences results in the remelting of LES and formation of AES. Additionally, the formation of AES is ascribed to the remelting of Ag-rich dendrite arms and growth of Cu-rich phases, as shown in Fig.14b. The supersaturated Cu element during solidification promotes partial remelting of Ag-rich dendrite arms, causing the dendrite skeleton of Ag-rich phase to be divided into several distinct particles. Subsequently, Cu-rich phases are nucleated and grow between adjacent dendrite arms of Ag-rich dendrites.

4.2.2 Ag-Cu-β ternary eutectic structures

In multicomponent alloys, a ternary eutectic structure, composed of three distinct phases, is usually formed during solidification, such as Al-Al_2Cu-Ag_2Al[78], Ag-Ge-ε_2[79], and Al_2O_3-YAG-ZrO_2 ternary eutectics[80]. The morphologies were reported to be lamellar, Chinese-script-like[80], chain-like, and non-chain-like patterns[78]. The addition of Sn, Ni, and In elements promoted the formation of Ag-Cu-(Ag, Cu)Zn ternary eutectic structure in Ag-Cu-Zn brazing filler metals and morphological transition[81]. However, the evolution of ternary eutectic structures in Ag based filler metals has been rarely reported, restricting the controlling of microstructures and properties of brazed joints.

Fig. 15 shows the morphologies of Ag-Cu-(Ag, Cu)Zn ternary eutectic structures after addition of Sn, Ni, and In elements with different contents. The white, gray, and black phases are Ag-rich, (Ag, Cu)Zn (β), and Cu-rich phases, respectively. The fraction of Cu-rich phases is lower than that of Ag-rich and β phases. The ternary eutectic structures consist of lamellar Ag-rich and β phases as well as discontinuous Cu-rich phases, and the arrangement of lamellae is irregular. Additionally, the dimension of Ag-rich phase is obviously larger than that of β and Cu-rich phases. This is attributed to the difficulty of nucleating Cu-rich phase from the liquid Ag based brazing filler metals[82]. With increasing the content of Sn (Fig.15a–15c), Ni (Fig.15d–15f), and In (Fig. 15g – 15i) elements, the dimension of Ag-rich phases decreases gradually, while the dimensions of β and Cu-rich phases do not change significantly. For the Ag-Cu-β ternary eutectic structures, the morphology of Cu-rich phase formed between Ag-rich and β phases is transformed from lamellae to irregular island with increasing the addition content of Sn, Ni, and In.

When the addition of Sn, Ni, and In elements in the brazing filler metals is low, an alternated and repeated arrangement of Ag/Cu/β/Ag/Cu/β ternary eutectic structure is formed in the Ag based brazing filler metals, as shown in Fig. 16a. The thickness of Cu-rich lamellae between Ag-rich and β phase is

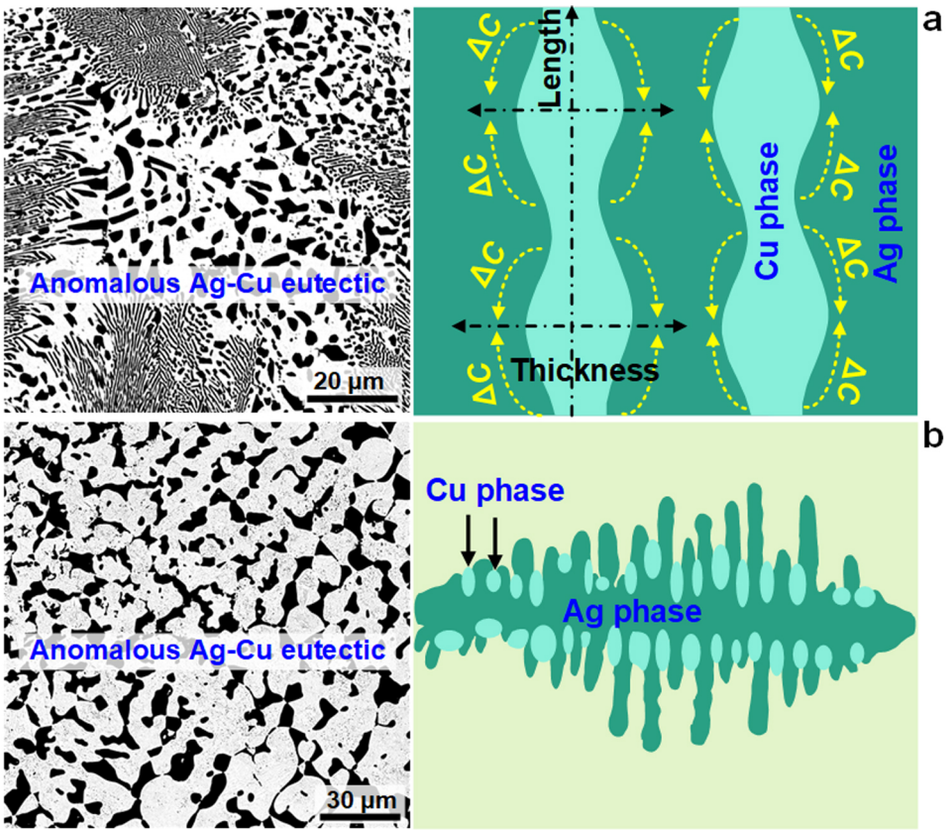

Fig.14 Morphologies and schematic diagrams of anomalous Ag-Cu eutectic structures transformed from lamellar eutectic structures (a) and Ag dendrites (b)

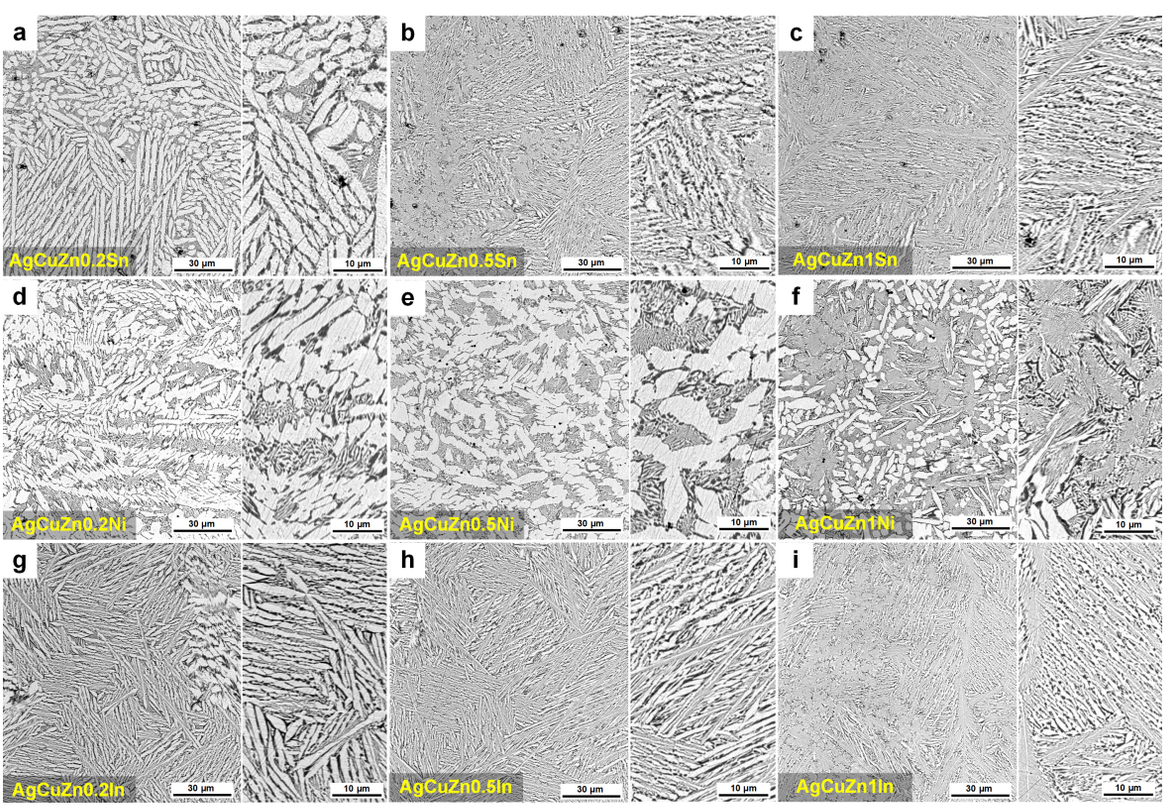

Fig.15 Microstructures and magnification of AgCuZn ternary eutectic structures after addition of Sn (a–c), Ni (d–f), and In (g–i) alloying elements with different contents

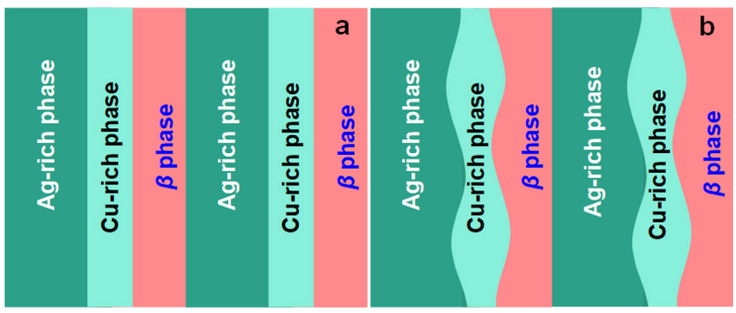

Fig.16 Schematic diagrams of growth of lamellar (a) and irregular (b) Ag-Cu-β ternary eutectic structures

thin. With increasing the Sn, Ni, and In addition contents, the solute concentration at the growth front of Ag-rich, Cu-rich, and β phases changes, generating oscillatory instability[83]. The oscillatory instability is characterized by the oscillation of the Cu-rich phase (Fig. 16b), changing the lamellar patterns with the presence of two mirror planes.

5 Conclusions

1) The design guidelines for composition of brazing filler metals encompass the designs of basic properties, manufacturability, and cost of brazing filler metals. The basic properties of brazing filler metals should include processability of brazing, mainly referring to the wettability and spreadability during brazing operations.

2) The constituent elements of brazing filler metals should be selected based on the elements in the base materials being joined. The selection rules refer to the metallurgical compatibility between elements in filler metals and base materials as well as and the melting temperature ranges of filler metals.

3) Integration design is the key to enhance the comprehensive properties of brazing filler metals, where binary or ternary eutectic systems and maximum solid solubility serve as guiding principles for ratios of element combination.

4) The determination principle for the primary elements ratio in brazing filler metals is approaching the eutectic composition, while balancing the advantages and disadvantages of hypoeutectic and hypereutectic alloys.

5) The addition of trace elements can effectively enhance the basic properties of brazing filler metals by modifying their phase composition. This requires consideration of new phases formed through reactions with the base material after brazing, as well as the new phases formed after the reaction between the brazing filler metals and base materials.

6) The design of processing technology and compositional design for brazing filler metals should be conducted synchronously, facilitating the conventional plastic forming as well as granulation and powder production.

7) The designed representative brazing filler metals have been successfully validated in applications including micro-nuclear power plants, aerospace engines, new radar systems, and thermonuclear fusion projects.

References

1 Long Weimin. *Journal of Iron and Steel Research International*[J], 2024, 31: 2327

2 Long Weimin, Li Shengnan, Du Dong *et al. Rare Metal Materials and Engineering*[J], 2019, 48(12): 3781

3 Long Weimin, Qiao Peixin, Zeng Daben *et al. Welding Technology*[J], 2002, 31(5): 33 (in Chinese)

4 Liu Xiaofang, Chang Yunfeng, Qinjian *et al. Welding*[J], 2024(12): 47 (in Chinese)

5 Si Hao, Qin Jian, Zhong Sujuan *et al. Rare Metal Materials and Engineering*[J], 2023, 52(3): 1027 (in Chinese)

6 Long Weimin, Sun Huawei, Baoli *et al. Welding Technology*[J], 2016(1): 59 (in Chinese)

7 Xia Yueqing, Ma Zhuang, Du Qiang *et al. Materials Characterization*[J], 2023, 207: 113520

8 Zhang Guanxing, Zhong Sujuan, Cheng Yafang *et al. Transactions of the China Welding Institution*[J], 2017, 38(12): 33 (in Chinese)

9 Zhao Jianchang, Lv Dengfeng, Long Weimin *et al. Welding*[J], 2016(5): 9 (in Chinese)

10 Liu Dashuang, Xu Jianhua, Li Xionghui *et al. Journal of Iron and Steel Research International*[J], 2024, 31: 2404

11 Jiang Nan, Zhang Liang, Sun Lei *et al. Rare Metal Materials and Engineering*[J], 2021, 50(1): 327 (in Chinese)

12 Huang Junlan, Long Weimin, Zhong Sujuan. *Journal of Mechanical Science and Technology*[J], 2020, 34(2): 711

13 Liu Han, Xue Songbai, Tao Yu *et al. Journal of Materials Research and Technology*[J], 2020, 9(6): 15908

14 Wei Li, Yao Jian, Zhang Jianting *et al. Rare Metal Materials and Engineering*[J], 2025, 54(2): 413

15 Liu Dashuang, Li Xionghui, Xu Jianhua *et al. Rare Metal Materials and Engineering*[J], 2025, 54(2): 394

16 Chen Guoqing, Yin Qianxing, Dong Zhibo *et al. Materials Characterization*[J], 2021, 171: 110781

17 Zhang Mingfen, Xu Shunjian, Valenza Fabrizio *et al. Journal of Advanced Ceramics*[J], 2025, 14(1): 9220997

18 Wu Jiangtao, Wang Ding, Huang Xingli *et al. Rare Metal Materials and Engineering*[J], 2025, 54(2): 319

19 Pan Yufan, Liang Jiabin, Nie Jialong *et al. Rare Metal Materials*

and Engineering[J], 2025, 54(2): 301

20 Liu Sixing, Liu Mingmiao, Liu Tianhong *et al. Wear*[J], 2023, 514–515: 204580

21 Habibi Farzad, Samadi Ahad, Nouri Mohammad. *International Journal of Refractory Metals and Hard Materials*[J], 2023, 116: 106354

22 Qu Hua, Song Kunlin, Zhang Lijiao *et al. Rare Metal Materials and Engineering*[J], 2025, 54(2): 445

23 Li Shengnan, Du Dong, Zhang Lei *et al. Reviews on Advanced Materials Science*[J], 2021, 60(1): 92

24 Long Fei, Liu Qu, Chen Gaoqiang *et al. Corrosion Science*[J], 2022, 208: 110675

25 Qin Jian, Dong Xian, Pei Yinyin *et al. Transactions of the China Welding Institution*[J], 2019, 40(8): 96 (in Chinese)

26 Shi Yinkai, Zhong Sujuan, Li Yunpeng *et al. Materials Science and Engineering A*[J], 2023, 886: 145690

27 Long Weimin, Lu Quanbin, He Peng *et al. Journal of Materials Engineering*[J], 2016, 44(6): 17 (in Chinese)

28 Xu Haitao, Li Yafei, Lu Chuanyang *et al. Journal of Nuclear Materials*[J], 2023, 581: 154439

29 Rawashdeh Rabeah Y, Qabaja Ghassan, Albiss Borhan Aldeen. *BMC Research Notes*[J], 2023, 16: 23

30 Liu Zhenwei, Wang Aiqin, Liu Pei *et al. Journal of Materials Research and Technology*[J], 2022, 18: 2354

31 Cui Li, Wu Defan, Ma Lixia *et al. Metallurgical and Materials Transactions A*[J], 2025, 56: 840

32 Yan Yanfu, Liu Jianping, Shi Yaowu *et al. Journal of Electronic Materials*[J], 2004, 33: 218

33 Li Yunpeng, Yu Hua, Shi Yinkai *et al. Materials Letters*[J], 2023, 330: 133269

34 Long Fei, Chen Gaoqiang, Zhou Mengran *et al. Journal of Magnesium and Alloys*[J], 2023, 11(6): 1931

35 Wang Lilin, Yang Fan, Gui Tianhong *et al. Materials Research Letters*[J], 2024, 12(9): 661

36 Wang Changwei, Jiang Wen, Han Kangning *et al. Engineering Failure Analysis*[J], 2024, 164: 108638

37 Huang Sen, Long Weimin, Lu Quanbin *et al. Materials Research Express*[J], 2019, 6: 056560

38 Sommer Ann-Kathrin, Turpe Matthias, Fussel Uwe. *Welding in the World*[J], 2020, 64: 1589

39 Tadashi Takemoto, Ikuo Okamoto, Junji Matsumura. *Transactions of JWRI*[J], 1987, 16(2): 301

40 Zhao J, Guo M, Hu S P *et al. Diamond and Related Materials*[J], 2020, 109: 108004

41 Mu Guoqian, Qu Wenqing, Zhang Yanhua *et al. Journal of Materials Science*[J], 2023, 58: 6297

42 Jafarlou D M, Zalnezhad E, Ezazi M A *et al. Materials & Design*[J], 2015, 87: 553

43 Zhao Zhanyong, Janasekaran Shamini, Fong Go Tze *et al. Metals and Materials International*[J], 2024, 30: 1743

44 Wiese S, Wolter K J. *Microelectronics Reliability*[J], 2004, 44(12): 1923

45 Johansson Jonas, Belov Ilja, Johnson Erland *et al. Microelectronics Reliability*[J], 2014, 54(11): 2523

46 Krupinski M, Krupinska B, Rdzawski Z *et al. Journal of Thermal Analysis and Calorimetry*[J], 2015, 120: 1573

47 Chuang T H, Yeh M S, Chai Y H. *Metallurgical and Materials Transactions A*[J], 2000, 31: 1591

48 Zhao Yijia, Jiu Yongtao, Liu Hao *et al. Materials Science and Engineering of Powder Metallurgy*[J], 2024, 29(4): 311 (in Chinese)

49 Lu Quanbin, Dong Xian, She Chun *et al. Transactions of the China Welding Institution*[J], 2018, 39(6): 53 (in Chinese)

50 Rajendran Sri Harini, Hwang Seung Jun, Jung Jae Pil. *Metals*[J], 2021, 11(3): 509

51 Niu Zhiwei, Huang Jihua, Liu Kaikai *et al. Materials Letters*[J], 2016, 179: 47

52 Long Weimin, Liu Dashuang, Qin Jian *et al. Journal of Adhesion Science and Technology*[J], 2023, 37(2): 319

53 Wang Xingxing, Li Shuai, Peng Jin. *Materials Research Express*[J], 2018, 5: 036506

54 Wang S S, Cheng M D, Tsao L C *et al. Materials Characterization*[J], 2001, 47(5): 401

55 Xue Peng, Zou Yang, He Peng *et al. Metals*[J], 2019, 9(2): 198

56 Ding Zongye, Yu Liao, Zhang Naifang *et al. Journal of Materials Science & Technology*[J], 2025, 209: 43

57 Long W M, Zhang G X, Zhang Q K. *Scripta Materialia*[J], 2016, 110: 41

58 Zhang Guanxing, Zhong Sujuan, Shen Yuanxun *et al. Transactions of the China Welding Institution*[J], 2023, 44(9): 37 (in Chinese)

59 Cao J, Zhang L X, Wang H Q *et al. Journal of Materials Science & Technology*[J], 2011, 27(4): 377

60 Wu Chuandong, Zhong Songqiang, Shen Shuai *et al. Journal of Alloys and Compounds*[J], 2025, 1011: 178410

61 Boettinger W J, Shechtman D, Schaefer R J *et al. Metallurgical and Materials Transaction A*[J], 1984, 15: 55

62 Basit Sercan, Esener Pinar Ata, Aydogan Yigit Yavuz *et al. Thermochimica Acta*[J], 2024, 740: 179828

63 Quan Mingsheng, Yan Zhiming, Liu Guilin *et al. Applied Physics A*[J], 2024, 130: 80

64 Wang X, Zhai W, Li H *et al. Acta Materialia*[J], 2023, 252: 118900

65 Cai Fangfang, Zhang Liangliang, Li Yunpeng *et al. Vacuum*[J], 2022, 201: 111066

66 El-Daly A A, El-Tantawy Farid, Hammad A E *et al. Journal of Alloys and Compounds*[J], 2011, 509(26): 7238

67 Cai Qing, Fang Changming, Mendis Chamini *et al. Journal of Alloys and Compounds*[J], 2023, 941: 168942

68 Delsante S, Novakovic R, Borzone G. *Journal of Alloys and Compounds*[J], 2018, 747: 385

69 Cline H E, Lee D. *Acta Metallurgica*[J], 1970, 18(3): 315

70 Ding Zongye, Long Weimin, Jiu Yongtao *et al. Crystals*[J], 2023, 13(1): 68
71 Qin Qingyuan, Li Jinfu, Yang Lin *et al. Materials Chemistry and Physics*[J], 2024, 311: 128521
72 Qin Qingyuan, Yang Lin, Li Jinfu. *Metallurgical and Materials Transactions A*[J], 2025, 56: 1171
73 Jackson K A, Hunt J D. *Transactions of The Metallurgical Society of AIME*[J], 1966, 236: 1129
74 Magnin P, Trivedi R. *Acta Metallurgica et Materialia*[J], 1991, 39(4): 453
75 Karma Alain, Sarkissian Armand. *Metallurgical and Materials Transactions A*[J], 1996, 27: 635
76 Galenko Peter K, Xu Junfeng. *Philosophical Transactions of the Royal Society A* [J], 2022, 380: 20200305
77 Zhao Su, Li Jinfu, Zhou Yaohe. *Journal of Alloys and Compounds*[J], 2009, 478: 252
78 Friess Jessica, Rayling Philipp, Hecht Ulrike *et al. Journal of Crystal Growth*[J], 2022, 595: 126799
79 Zhai Wei, Hong Zhenyu, Mei Cexiang *et al. Science China-Physics, Mechanics & Astronomy*[J], 2013, 56(2): 462
80 Lee Jong Ho, Yoshikawa Akira, Fukuda Tsuguo *et al. Journal of Crystal Growth*[J], 2001, 231: 115
81 Dimitrijevic Stevan P, Manasijevic Dragan, Kamberovic Zeljko *et al. Journal of Materials Engineering and Performance*[J], 2018, 27(4): 1570
82 Kabassis H, Soda H, Rutter J W *et al. Canadian Metallurgical Quarterly*[J], 1981, 19(4): 345
83 Choudhury Abhik, Plapp Mathis, Nestler Britta. *Physical Review E*[J], 2011, 83: 051608

钎焊材料成分设计准则及典型组织演变机制

龙伟民
(中国机械总院集团郑州机械研究所有限公司 高性能新型焊接材料全国重点实验室，河南 郑州 450052)

摘 要：钎焊材料应用广泛，在异质结构连接中发挥着工业万能胶的作用。新结构和新材料层出不穷，所需要的新型钎焊材料越来越多。研究钎料成分优化设计方法，形成钎料系统性设计准则意义重大。从应用钎料基本性能、成形加工性和综合成本三维视角出发，阐明了钎料成分设计的基本规则。本研究中钎料本构性能包括钎料机械性能、物理化学性能、电磁性能、耐蚀性能与钎焊作业时钎料的润湿性和流铺性。成型加工性包括熔炼、铸造工艺，挤压、轧制、拉拔、制环工艺，制粒、制粉和非晶微晶成型工艺。成本指材料价值和制造成本之和。提高钎料综合性能需要全面系统考量设计指标，突出钎料特色要聚焦相应技术指标，二元或三元共晶组织可以有效提高钎料流铺性，固溶体组织有利于钎料成形。采用所提出的设计准则，设计了典型的Ag基、Cu基、Zn基、Sn基钎料，并在重大科学工程中得到成功应用。

关键词：钎料设计；成分设计准则；银钎料；共晶组织演变

作者简介：龙伟民，男，1966年生，博士，研究员，中国机械总院集团郑州机械研究所有限公司高性能新型焊接材料全国重点实验室，河南 郑州 450052，E-mail：longwm@zrime.com.cn